FULL PAPER

Controlled Microfabrication of High-Aspect-Ratio Structures in Silicon at the Highest Etching Rates: The Role of H_2O_2 in the Anodic Dissolution of Silicon in Acidic Electrolytes

*Chiara Cozzi, Giovanni Polito, Kurt W. Kolasinski, and Giuseppe Barillaro**

In this work the authors report on the controlled electrochemical etching of high-aspect-ratio (from 5 to 100) structures in silicon at the highest etching rates (from 3 to 10 μm min^{-1}) at room temperature. This allows silicon microfabrication entering a previously unattainable region where etching of high-aspect-ratio structures (beyond 10) at high etching rate (over 3 μm min^{-1}) was prohibited for both commercial and research technologies. Addition of an oxidant, namely H_2O_2, to a standard aqueous hydrofluoric (HF) acid electrolyte is used to dramatically change the stoichiometry of the silicon dissolution process under anodic biasing without loss of etching control accuracy at the higher depths (up to 200 μm). The authors show that the presence of H_2O_2 reduces the valence of the dissolution process to 1, thus rendering the electrochemical etching more effective, and catalyzes the etching rate by opening a more efficient path for silicon dissolution with respect to the well-known Gerischer mechanism, thus increasing the etching speed at both shorter and higher depths.

1. Introduction

Since the famous talk of R. Feynman in 1959 "There is plenty of room at the bottom," silicon microstructuring technologies have been continuously developed with the ambition of sculpting silicon at the microscale, thus pushing silicon toward novel research topics and market opportunities beyond Moore's law, a trend also known as More Than Moore.[1,2] As a result, silicon microoptoelectromechanical systems (e.g., pressure sensors, accelerometers, gyroscopes) are nowadays an integral component of virtually any of the sophisticated devices (e.g., mobile phones, cars, videogames, airplanes) of everyday life.[3–5] On the other hand, lab-on-a-chip systems integrating a multitude of micrometer-sized components on a silicon chip (e.g., microneedles, microchannels and valves, biosensors) are on the way and will radically transform clinical diagnostics and medicine.[6,7] Finally, emerging applications in microelectronics, e.g., through silicon vias for 3D chip stacking and 3D capacitors with dramatically enhanced value for unit area, are among the new critical challenges that silicon microstructuring technologies are facing today.[8,9] Both these applications require the development of novel high-aspect-ratio structures that are well beyond values attainable by commercial technologies (aspect ratio AR < 40). On the other hand, state-of-the-art technologies able to control microfabrication at higher aspect-ratios (AR > 100) are limited in terms of etching rate, which is usually restricted to below 2 μm min^{-1} when the aspect-ratio increases over 20.

Figure 1 groups experimental data on etching rate versus aspect-ratio value typical of the principal commercial and research microfabrication technologies, according to authors' best knowledge. Prior results define an unattainable region that is inaccessible for silicon microfabrication technologies, either at commercial or research level (gray area in Figure 1). Its boundary is quite reasonably well described by a power law $ER = a\,AR^b$, as estimated from experimental data available on the different microfabrication technologies, where ER is the growth rate in μm min^{-1}, AR is the aspect ratio, and a and b are fitting parameters (a = 23.9 μm min^{-1} and b = −0.55 on the basis of data available on Figure 1).

Time-multiplexed etching (TMEP) process, also known as Bosch process, is the leading microfabrication technology at industrial level.[10] It relies on alternating etching and passivation (polymerization) steps, e.g., using SF_6 as etch gas and C_4F_8 and Ar as polymerization gases. In spite of TMEP being highly reliable and greatly flexible, TMEP features an aspect-ratio dependent etching rate (ARDE).[11] ARDE usually limits AR of microfabricated pores in the range from 1 to 16 at etching rates from 6 to 3 μm min^{-1}, respectively (black stars in Figure 1). Although ARDE is less restrictive for trenches, their aspect ratio is also limited to a maximum value of 21 at etching rate of about 4 μm min^{-1} (green squares in Figure 1).

Metal-assisted chemical etching (MaCE) is a novel microfabrication technology that allows targeting AR of 30 though at etching rate <1 μm min^{-1} (red upside-down triangles in Figure 1).[12–14] MaCE makes use of HF–H_2O_2 solutions to catalyze chemical silicon dissolution in correspondence with noble metal (e.g., Pt, Au) sites patterned on the silicon

C. Cozzi, G. Polito, Prof. G. Barillaro
Dipartimento di Ingegneria dell'Informazione
Università di Pisa
via G. Caruso 16, 56122 Pisa, Italy
E-mail: g.barillaro@iet.unipi.it
Prof. K. W. Kolasinski
Department of Chemistry
West Chester University
West Chester, PA 19383, USA

DOI: 10.1002/adfm.201604310

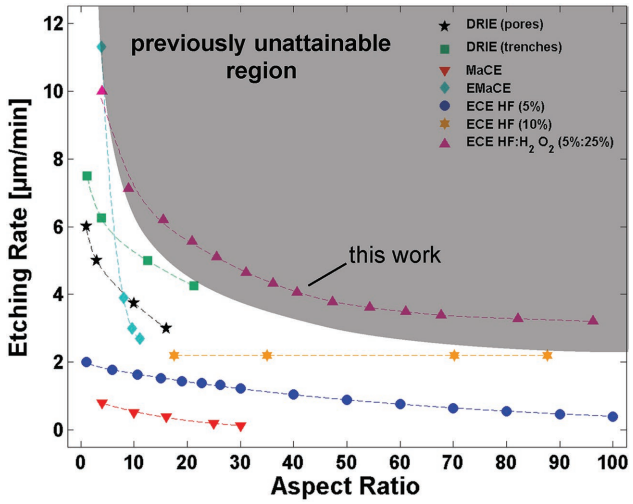

Figure 1. Figure of merit of main silicon micromachining technologies. Comparison between this work and commercial/state-of-the-art silicon microfabrication technologies, namely deep reactive ion etching (DRIE),[10] metal-assisted chemical etching (MaCE),[12,13] electric bias-attenuated MaCE (EMaCE),[15] electrochemical etching (ECE) at [HF] of 5% and 10%,[21] in terms of etching rate (ratio between etch depth and etch time [µm min^{-1}]) versus aspect ratio (ratio between the depth of in-silicon vertical feature and its width). The Figure highlights as this work allows silicon microfabrication entering the previously unattainable region for aspect-ratio values in the range 10–100.

surface. Although largely used at research level, the low etching rate (about ten times lower that TMEP processes) hinders MaCE application to large-scale manufacturing. An electric bias-attenuated metal-assisted chemical etching (EMaCE) was recently reported that enhances the etching rate of MaCE to 11.3 µm min^{-1} at AR of 4 (cyan diamonds in Figure 1).[15] EMaCE exploits electrical biasing of the silicon substrate to focus holes responsible for initiation of silicon dissolution underneath the metal catalyst, thus improving both etching control and speed. Still, the EMaCE etching rate decreases rapidly with aspect ratio, with a value of about 2.7 µm min^{-1} at AR of 11.

Silicon electrochemical etching (ECE) is a well-known technology for microfabrication of both ordered pores[16,17] and complex systems[18,19] with high aspect ratio. In spite of many advantages[18,19] (e.g., surface roughness, in-plane and out-of-plane uniformity, anisotropy control, aspect ratio) of ECE technology with respect to other microstructuring approaches, a number of limitations[20] (e.g., etching rate, maximum/minimum size, and spacing) still exist that need to be addressed toward commercial applications. Back-side illumination is used to focus holes specifically to defects patterned on the surface of n-type silicon wafers and enable, in turn, controlled dissolution in aqueous HF (5 vol%) electrolytes under anodic biasing. AR values over 100 are obtained for ordered pores and systems with micrometric features, though the etching rate (about 2 µm min^{-1} at low AR) reduces to 0.5 µm min^{-1} at the highest ARs (blue circles in Figure 1). Increasing the HF concentration from 5 to 10 vol% allowed maintaining the etching rate constant at 2.2 µm min^{-1} regardless of the AR value, in the range from 17 to 88 (orange hexagrams in Figure 1).[21] However, only pore fabrication (no microstructures) has been demonstrated with such an increased HF concentration.

Summarizing, silicon technologies, either wet or dry, are strongly limited by diffusion of reactive species within narrow and deep pores, which limits the fabrication of high AR pores at high etching rate. Diffusion of chemical species within the pores (i.e., Fick's law) as well as removal of reaction byproducts from the pores is responsible for such a reduced etching rates as AR increases. A necessary trade-off among concentration of reactive species, removal of chemical byproducts, and flexibility and control on the etching process has set this boundary so far.

In this work we report on a micromachining technology able to enter the previously unattainable region in Figure 1 (cyan triangles). More in detail, we enable the controlled electrochemical etching of high-aspect-ratio (from 5 to 100) structures in silicon at the highest etching rates (from 3 to 10 µm min^{-1}), at room temperature using a low HF concentration (5 vol%). This sets a novel record among either commercial or state-of-the-art silicon etching technologies. We show that the addition of an oxidant, namely H_2O_2, to a standard aqueous HF electrolyte facilitates a dramatic change in the stoichiometry of the silicon dissolution process under anodic biasing without loss of etching control accuracy at the higher depths (up to 200 µm). The presence of H_2O_2 acts both in dropping the valence of the silicon dissolution process to 1, thus rendering the electrochemical etching more effective, and in catalyzing the etching rate by opening a more efficient path for silicon dissolution with respect to the well-known Gerischer mechanism,[22,23] thus increasing the etching speed at both shorter and higher depths.

2. Results and Discussion

2.1. Controlled High-Speed Electrochemical Etching at High Aspect Ratio of Regular Macropores and Microstructures in n-Type Silicon in Aqueous HF–H_2O_2 Electrolytes

Figure 2 shows scanning electron microscope (SEM) cross-section images of regular arrays of macropores electrochemically etched under back-side illumination at anodic voltage of 1.2 V in two aqueous electrolytes containing [HF] = 5% with H_2O_2 at concentration of 25% (Figure 2a,c) and without H_2O_2 (used as control) (Figure 2b,d), at two etching times, namely 10 and 60 min. The control electrolyte (without H_2O_2) was a well-known mixture of HF:H_2O (5%:95%, v/v) commonly employed for the electrochemical etching of both regular macropores[16,17] and complex microstructures[18,19] in n-type silicon electrodes at low anodic voltage under back-side illumination. Remarkably, macropores etched for 10 min in the electrolyte with [H_2O_2] = 25% feature a mean depth of 48.99 µm (standard deviation sd = 0.07 µm), which corresponds to an average etching rate over 10 min of about 5 µm min^{-1}. The average etching rate with [H_2O_2] = 25% was about 2.8 times larger than that of the control electrolyte (without H_2O_2) for which shorter macropores with depth of only 18.45 µm (sd = 0.25 µm) were etched in the same time (about 1.8 µm min^{-1}), in agreement with the current literature.[24] By increasing the etching time to 60 min, macropores with mean depth of 177.93 µm (sd = 0.37 µm) were etched using the electrolyte with [H_2O_2] = 25%, whereas macropores

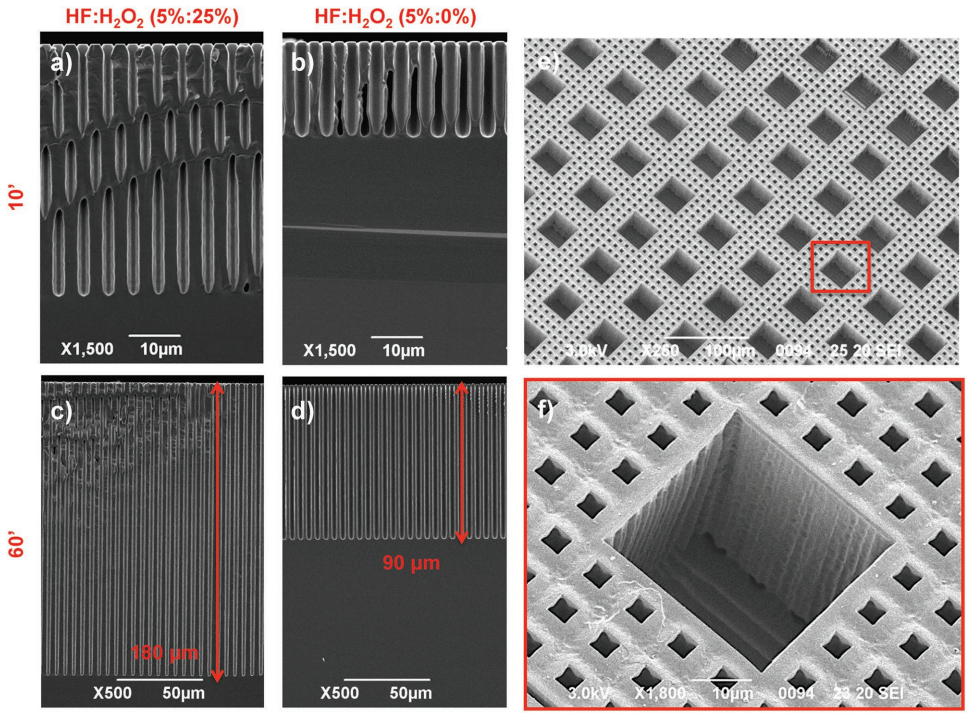

Figure 2. Effect of the addition of H_2O_2 to HF-aqueous electrolyte on the fabrication of regular macropore arrays in silicon by electrochemical etching. SEM cross-section of regular macropore arrays etched under back-side illumination for a,b) 10 and c,d) 60 min at 1.2 V and etching current density of 36.49 mA cm^{-2} a,c) in the presence of [HF] = 5%-based electrolyte with [H_2O_2] = 25% and b,d) without H_2O_2 (control). The significant increase of the etching rate by addition of H_2O_2 to the control electrolyte is appreciable. e,f) SEM bird-views of a silicon microstructure that integrates a 2D array of holes with depth of 50 µm and different aspect ratios (namely, 1 and 10) on the same silicon die, fabricated in 10 min at 3 V and 60 mA cm^{-2} in the presence of [HF] = 5%-based electrolyte with [H_2O_2] = 25%. Noteworthy, the possibility of control the etching anisotropy in real-time and fabricate complex microstructures is retained at high etching rates.

etched with the control electrolyte feature a mean depth of 90.38 µm (sd = 0.59 µm). The average etching rate over 60 min in the electrolyte with [H_2O_2] = 25% was about 3 µm min^{-1}, which was two times larger than that in the control electrolyte (about 1.5 µm min^{-1}). It is important to note that the etching rate was evaluated as the ratio between etch depth and etch time. On the basis of these experimental results, we can assert that the presence of [H_2O_2] = 25% in the electrolyte during silicon electrochemical etching facilitates significant enhancement of the silicon etching rate and, in turn, macropore growth rate, at any depth with respect to the control electrolyte (without H_2O_2). Nonetheless, reduction in the etching rate from about 5 µm min^{-1} at a depth of 50 µm to about 3 µm min^{-1} at a depth of 180 µm clearly indicates that the diffusion kinetics of active species, i.e., HF and H_2O_2, to the active site of reaction, i.e., the macropore tip, still plays a major role in the electrochemical dissolution of silicon over depth.[16,24]

Remarkably, the enhancement of the etching rate in the presence of H_2O_2 does not negatively affect macropore quality (e.g., in terms of surface roughness, pore diameter control, or their dependence on depth) with respect to macropores etched in control electrolyte (Figure S1 and S2, Supporting Information). From SEM analysis of macropore cross-sections no appreciable difference in either surface roughness or diameter variation over depth was observed in the presence of H_2O_2 with respect to the control solution. In particular, Figure S2 in the Supporting Information allows appreciation of the presence of a microporous layer covering the inner sidewall surface of pores etched both in the control electrolyte and in the presence of H_2O_2. No microporous layer is visible at the very pore tip, in agreement with the Lehmann model for which $J_{tip}(\theta) = J_{tip}\cos(\theta)$, being J_{tip} the current density value at the pore tip and θ the angle formed between axes of the pore and a line perpendicular to the surface of the pore ($\theta = 0$ at the very pore tip and becomes 90° at the pore sidewall).[16]

Moreover, the peculiarity of the electrochemical etching technology enabling fabrication of complex microstructures at high AR value with high accuracy by modulation in real-time of the etching anisotropy[18,19] is also retained at such high etching rates. Figure 2e,f shows SEM bird-views of a silicon microstructure that integrates a 2D array of square holes with sides of about 40 µm and spatial periods of 70 µm together with a 2D array of square pores with sides of about 4 µm and spatial periods of 10 µm. The larger square holes were obtained through the use of sacrificial structures that were removed by switching the etching from the anisotropic to the isotropic regime.[18] Both arrays feature a depth of about 50 µm after an etching time of 10 min in a [HF] = 5% electrolyte with [H_2O_2] = 25%. An etching time of 35 min is needed to fabricate the same microstructure using the control electrolyte.[25] The etching depth is in good agreement with depth of regular macropore arrays in Figure 1a. The microstructure combines on the same die low (about 1) and high (about 10) AR holes etched at an average rate of 5 µm min^{-1}. Quality of microfabrication and

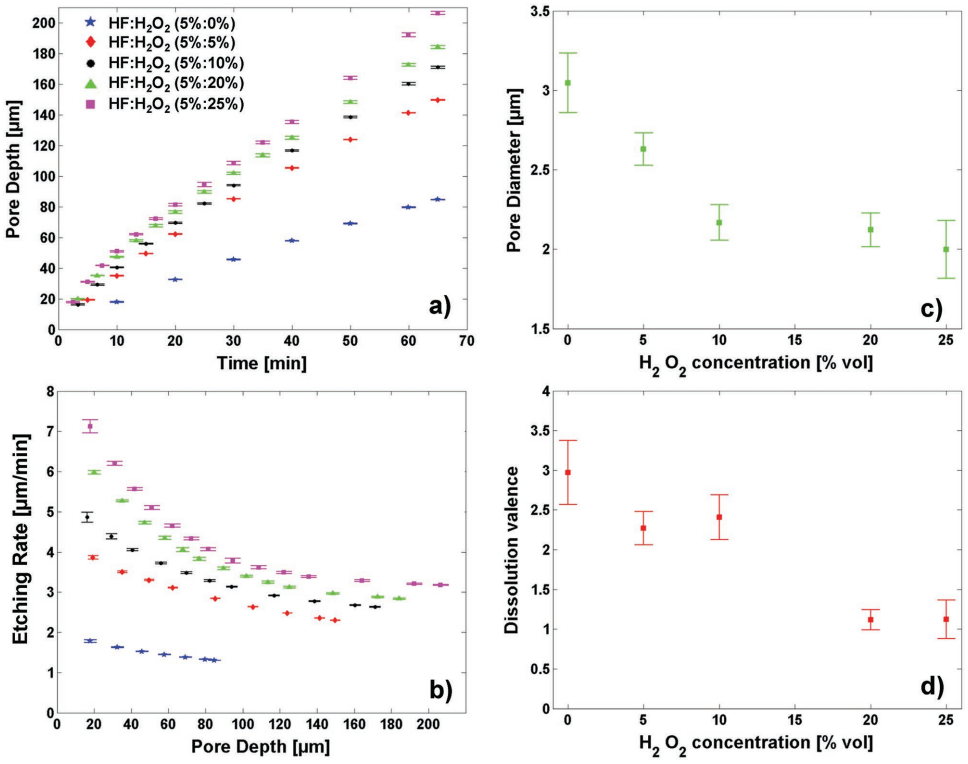

Figure 3. Effect of the H_2O_2 concentration within HF-aqueous electrolyte on depth and etching rate of regular macropore arrays fabricated in silicon by electrochemical etching. Experimental data on a) depth (average value and standard deviation) versus time and b) etching rate (average value and standard deviation) versus depth of regular macropore arrays etched at 1.2 V and etching current density of 36.49 mA cm^{-2} in the presence of [HF] = 5%-based electrolyte with different H_2O_2 concentrations (i.e., 0%, 5%, 10%, 20%, 25%); experimental data on c) pore diameter and d) dissolution valence of regular macropore arrays, etched in the same conditions above reported, as a function of the $[H_2O_2]$ concentration. Remarkably, the dissolution valence of pores etched in the presence of H_2O_2 at concentration of 25% is lowered to 1.

surface roughness are comparable to those obtained using the control electrolyte.[25] Figure S3 in the Supporting Information shows a top view of the microstructure in Figure 2e,f with a sacrificial structure sitting on top, which allows appreciation of the low surface roughness resulting from the etching process.

To gain insight into the effect of addition of H_2O_2 to the control electrolyte on the silicon dissolution process, regular macropore etching in n-type silicon under back-side illumination was investigated for different H_2O_2 concentrations ($[H_2O_2]$ = 0%, 5%, 10%, 20%, 25%) as a function of the etching time (from 0 to 65 min). Regardless of the electrolyte composition, all experiments were carried out with same initial etching parameters, and etching current density was adjusted over time to keep the pore diameter constant over depth, as detailed in the Experimental Section. For a given H_2O_2 concentration an experimental growth curve linking macropore depth and etching time was recorded by using a labeling methodology. This latter method allows marking the macropore growth over time on a single silicon sample using a time-pulse modulation of the etching current density (Figure S4a, Supporting Information), as detailed in the Supporting Information. Preliminary experiments were carried out with the control electrolyte and with an electrolyte containing $[H_2O_2]$ = 5% aimed at validating the effectiveness of the labeling methodology with respect to the standard methodology, for which a new experiment is required for any different etching time. Outcomes of these experiments (Figure S4, Supporting Information) confirm that pore growth curves obtained by using the two methodologies are identical within the experimental error (Figure S4c, Supporting Information).

Figure 3a shows experimental growth curves (mean value and standard deviation) of regular macropores electrochemically etched in n-type silicon under back-side illumination up to 65 min using aqueous HF-based electrolytes without (control) and with H_2O_2 at concentrations in the range from 5 to 25 vol%.

From Figure 3a it is immediately apparent that: (1) for any tested electrolyte the pore depth consistently increased with etching time; (2) for any etching time the etching depth consistently increased with H_2O_2 concentration in the electrolyte. The growth curves for both control electrolyte and electrolyte with $[H_2O_2]$ = 25% are in good agreement with the results of experiments reported in Figure 2. The higher H_2O_2 concentration in the electrolyte enabled the etching of about 200 µm deep regular macropores with aspect-ratio of about 100 in roughly 1 h, thus breaking new ground in the silicon micromachining arena. For comparison, etching of regular macropores with the same depth using control electrolyte takes about 4 h.

Figure 3b shows experimental data on the etching rate (in µm min^{-1}) versus depth of regular macropores as a function of the H_2O_2 concentration in the electrolyte. It is apparent that the control electrolyte ($[H_2O_2]$ = 0%) has a maximum etching rate

of about 2 μm min^{-1} for smaller etching depth (<20 μm) that decreases with depth due to HF diffusion within the pores and tends to a limiting value below 1 μm min^{-1} at higher etching depth (>80 μm), in agreement with literature data.[24] Conversely, by increasing the concentration of H_2O_2 in the electrolyte it is possible to monotonically and significantly increase the etching rate both at the smaller and higher depths, with respect to the control electrolyte (Figure S5a,b, Supporting Information). Indeed, at smaller depth (≤20 μm) the macropore etching rate is higher than 7 μm min^{-1} and decreases to about 3 μm min^{-1} at higher etching depth (≥200 μm), in the presence of [H_2O_2] = 25%. In agreement with the trend in Figure 3a,b, macropores with depth of 10 μm were etched in 1 min at H_2O_2 concentration of 25%, which corresponds to an etching rate of 10 μm min^{-1}. Figure S5c, Supporting Information highlights the significant increase of the etching rate versus aspect ratio of etched pores in the presence of H_2O_2, which results to be greater than 7 μm min^{-1} at AR < 10, with a maximum value of 10 μm min^{-1} at AR = 5. As the H_2O_2 in the electrolyte increases, there is a dramatic increase of the etching rate for any aspect ratio, with respect to the control electrolyte. It is worth noting that: (1) addition of [H_2O_2] = 5% to the control electrolyte is enough to roughly double the macropore growth rate both at the smaller and higher depths, with respect to the control electrolyte itself; (2) addition of [H_2O_2] = 10%, 20%, and 25% to the control electrolyte allows increasing the macropore growth rate respectively 2.7, 3.6, and 4 times at the smaller depth, and 2, 2.2, and 2.4 times at the higher depth, with respect to the control electrolyte itself; (3) electrolytes containing H_2O_2 feature a growth rate at the higher depth that is always higher than that of the control electrolyte in spite of the lower depth of macropores etched for the latter, regardless of the H_2O_2 concentration.

To gain a deeper understanding of the effect of H_2O_2 on the electrochemical dissolution of silicon in HF-aqueous electrolytes, diameter of etched ordered macropores (Figure 3c) and dissolution valence of electrochemical etching process (Figure 3d) were investigated as a function of the H_2O_2 concentration.

The diameter of macropores etched in electrolyte with [H_2O_2] = 25% had an average value of 1.99 μm (sd = 0.18 μm), whereas macropores etched in the control electrolyte featured an average diameter of 3.05 μm (sd = 0.19 μm), which was about 1.5 times larger and in agreement with literature data.[26] This means that the presence of [H_2O_2] = 25% in the electrolyte during anodic dissolution of silicon enhances macropore etching rate in the out-of-plane direction with respect to the in-plane direction, if compared with control electrolyte, which is consistent with the etching of deeper macropores with smaller diameter.

The dissolution valence, by definition the number of charge carriers required for the dissolution of a single silicon atom, of the electrochemical etching process in the presence of [H_2O_2] = 25% had an average value of 1.12 (sd = 0.24), whereas the dissolution valence with the control electrolyte had an average value of 2.97 (sd = 0.40), which is in good agreement with literature data.[24] Remarkably, the dissolution valence decreased as the H_2O_2 concentration in the electrolyte increased, thus corroborating the hypothesis that the oxidant agent, namely H_2O_2, was able to promote a change in the stoichiometry of silicon dissolution process by consuming conduction band electrons.[27] Note further that the reduction in valence stands in contradiction to the current burst model[28] prediction of an increase in the dissolution valence with increasing oxidant concentration. This model predicts that the presence of an oxidant should enhance the contribution of a valence 4 process, which we obviously do not observe.

Further experiments were carried out to investigate the effect on the etching rate of increasing HF concentrations in the presence of H_2O_2. It is known that using a standard HF:H_2O electrolyte, the etching rate of macropores in n-type electrodes under anodic biasing and back-side illumination is governed by the following equation

$$ER = \frac{J_{tip}}{n_v e N_{Si}} \tag{1}$$

where n_v is the dissolution valence, e the elementary charge, and N_{Si} the atomic density of silicon.[16,24] The electropolishing current density value at the pore tips J_{tip} mainly depends on both HF concentration C_{tip} and temperature T at the pore tips according to the following equation

$$J_{tip} = a C_{tip}^{b} exp\left(\frac{E_a}{kT}\right) \tag{2}$$

where a and b are suitable constants, E_a is the activation energy, k is the Boltzmann constant, and T is the temperature.[16,24] The following simplified expression for C_{tip}

$$C_{tip} = C_0 \frac{\left(1+\frac{x_p}{2c}\right)}{\left(1+\frac{3x_p}{2c}\right)} \tag{3}$$

can be retained for most practical cases, where c is a suitable constant and x_p is the pore depth.[24] Equation (3) points out that C_{tip} depends nonlinearly on the bulk HF concentration C_0 on flat electrodes and decreases as the macropore depth increases.

From Equations (1) to (3) it is clear that the etching rate of macropores in n-type silicon can be increased, in principle at least, by increasing both operation temperature T and HF concentration. In order to obtain the highest microfabrication quality, it is essential to keep the operating temperature as low as possible in order to optimize etching of both macropores and microstructures. The use of low temperature avoids isotropic electron–hole pair generation in silicon between etched features that gives rise to the etching of secondary pores (a phenomenon known as branching).[16] Therefore, further experiments were conducted at room temperature though increasing the HF concentration. All experiments were carried out for an etching time of 10 min, with HF concentrations ranging from 5% to 8% and H_2O_2 concentrations ranging from 0% to 15%. Figure S6 in the Supporting Information summarizes experimental data on macropore growth rate obtained at increasing HF concentration in the presence of H_2O_2. It is apparent that the increase of the HF concentration leads to an augmented etching rate for any tested H_2O_2 concentration. For

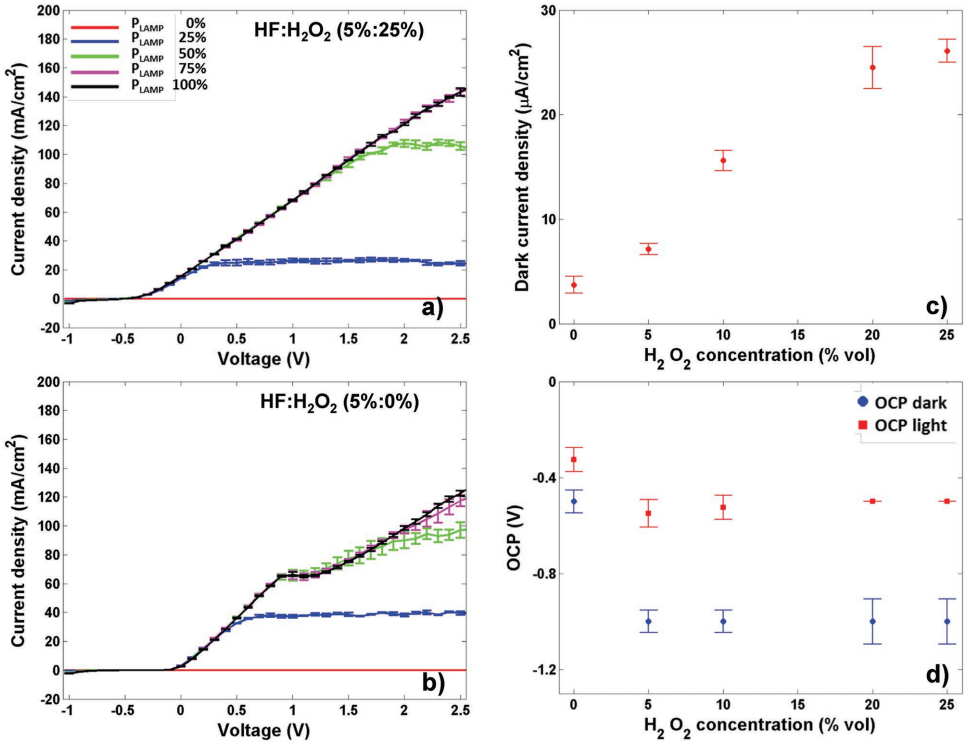

Figure 4. Investigation of the effect of H_2O_2 concentration within HF-aqueous electrolyte on the silicon dissolution process. Experimental current density–voltage curves (average value and standard deviation) of n-type silicon electrodes a) in the presence of two different [HF] = 5%-based electrolytes with $[H_2O_2]$ = 25 vol% and b) without H_2O_2 (control), both in dark and under back-side illumination; c) current density value in dark and d) open-circuit potential value as a function of the $[H_2O_2]$ concentration, both in dark and under illumination of the silicon electrode.

a given H_2O_2 concentration, the higher the HF concentration the higher is the growth rate. For instance, for $[H_2O_2]$ = 15% macropore etching rate increases from 4 μm min^{-1} at [HF] = 5% to about 7 μm min^{-1} at [HF] = 8%. A power law dependence of the growth rate on the HF concentration is found regardless of the H_2O_2 concentration value, in agreement with Equations (1) and (2).

2.2. Current Density–Voltage Curves of n-Type Silicon Electrodes in Aqueous HF–H_2O_2 Electrolytes

Figure 4a,b shows typical experimental current density–voltage (*J–V*) curves (average value and standard deviation) of n-type silicon electrodes in the presence of the two electrolytes with the same [HF] = 5% though different $[H_2O_2]$, namely 25% (Figure 4a) and 0% (control) (Figure 4b). The *J–V* curves were recorded around the open-circuit-potential (OCP) region between –1 and +2.5 V at different illumination intensity values obtained by tuning the lamp power from 0% to 100%. The *J–V* curves mostly refer to the anodic region of the silicon/electrolyte system, because silicon dissolution in HF-based electrolytes only occurs under anodic biasing. *J–V* curves referring to the other electrolytes under investigation, with H_2O_2 concentration between 5% and 20%, are reported in Figure S7 in the Supporting Information.

From the *J–V* curves of Figure 4a,b it is apparent that, regardless of the presence of H_2O_2, the silicon/electrolyte system was reverse-biased under anodic voltage and the use of back-side illumination of the silicon electrode allowed for fine control of the etching current density flowing through the silicon/electrolyte junction.

In dark condition (red curves in Figure 4a,b) only a small current density flowed through the silicon/electrolyte junction, with an average value increasing with the H_2O_2 concentration, from 3.7 μA cm^{-2} (sd = 0.8 μA cm^{-2}) in the control electrolyte to 26.1 μA cm^{-2} (sd = 1.1 μA cm^{-2}) for the electrolyte with $[H_2O_2]$ = 25% (Figure 4c). The current density value recorded in dark condition with the control electrolyte (without H_2O_2) was in good agreement with data reported in the literature[29,30]: the slow charge injection from fluoride ions (F^-) during silicon etching determined its low value. The addition of different concentrations of H_2O_2 to the control electrolyte increased current density values in dark and, in turn, charge injection by a factor of 7 (Figure 4c), though its value was still extremely low in comparison with charge injection recorded under back-side illumination (from blue to black curves in Figure 4a). We argue that the direct charge injection from H_2O_2 into the Si valence band makes a negligible contribution to the current that flows during etching.

Under illumination of the silicon electrode (blue, green, magenta, and black curves in Figure 4a,b), the electrical current flowing through the silicon/electrolyte junction significantly increased thanks to the contribution of holes photogenerated at the back-side silicon surface and collected at the silicon/electrolyte interface. Under high illumination intensity (≥50%

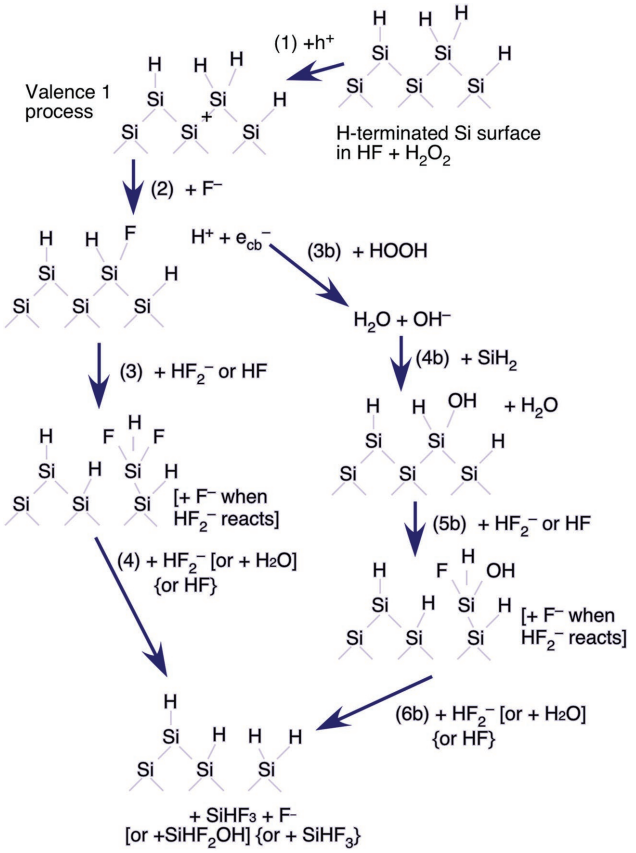

Figure 5. A schematic representation of the standard Gerischer mechanism augmented by H_2O_2 assisted etching of Si. The series of steps along the left hand column corresponds to the Gerischer mechanism. Etching is always initiated by hole injection into the valence band. However, in the presence of H_2O_2, a second etching pathway opens up (the right hand pathway) in which the electron injected into the conduction band by F^- is captured by H_2O_2. This liberates OH^- at the surface, which induces further etching through base-catalyzed hydrolysis. Both reactions, when performed separately, are known to yield hydrogen-terminated surfaces after Si atom removal.

of the lamp power), a typical electropolishing current density peak J_{ep} = 66.45 mA cm^{-2} at anodic voltage of V_{ep} = 1 V was clearly visible with the control electrolyte (Figure 4b), beyond which the current density increased almost linearly with anodic voltage.[16] Conversely, as the H_2O_2 concentration in the electrolyte increased from 5% to 25%, on the one hand, the electropolishing current density peak did not show up anymore (being already barely visible with 5% of H_2O_2) and the current density linearly increased with the anodic voltage until saturation (Figure 4a and Figure S7a–c, Supporting Information); on the other hand, under high illumination intensity (≥50% of the lamp power) the slope of the current density–voltage curves (dJ/dV) decreased as the H_2O_2 concentration increased (Figure S7d, Supporting Information), thus confirming that H_2O_2 was unable to significantly inject charges into silicon during etching.

We argue in the next section that the ability of the oxidant (i.e., H_2O_2 in this case) to change the stoichiometry of anodic silicon dissolution is related to its ability to consume the conduction band electrons produced in the second step of the well-known Gerischer mechanism.[22] It can also explain the reduction of the current density–voltage curves slope (dJ/dV) as H_2O_2 concentration increased: H_2O_2 molecules scavenge conduction band electrons, which are then not measured, to generate hydroxide ions (OH^-), well known to catalyze the reaction of H_2O with silicon.[31,32]

The OCP value was also dependent on the presence of H_2O_2 in the electrolyte, both in dark and under illumination conditions, as shown in Figure 4d. In dark condition, the OCP value exhibited a clear cathodic shift in the presence of H_2O_2, from –0.5 V (sd = 0.05 V) for the control electrolyte to –1 V (sd = 0.09 V) for the electrolyte with [H_2O_2] = 25%, with no significant dependence on the H_2O_2 concentration. Under illumination, the OCP value showed an anodic shift with respect to dark condition, from –0.5 V (sd = 0.05 V) to –0.325 V (sd = 0.05 V) for the control electrolyte and from –1 V (sd = 0.09 V) to –0.5 V (sd = 0.0005 V) for the electrolyte with [H_2O_2] = 25%, in agreement with the literature.[33] Moreover, under illumination, the OCP value exhibited a cathodic shift as H_2O_2 concentration increased in the electrolyte, from –0.325 V of the control electrolyte (OCP_0) to –0.5 V for the electrolyte with [H_2O_2] = 25% (OCP_{25}). The cathodic OCP shift value ($\Delta OCP = OCP_{25} - OCP_0$) is equal to –0.175 V, which means that the Fermi level is shifting up in energy by +0.175 V. We argue that addition of H_2O_2 lowers the band bending of 0.175 V in silicon/electrolyte band diagram, in good agreement with the literature.[34]

2.3. Dissolution Mechanism of n-Type Silicon in Aqueous HF–H_2O_2 Electrolytes

We have demonstrated that the rate of anodic etching in acidic fluoride solutions is enhanced by the presence of H_2O_2 in the electrolyte. In the previous section we proposed that this enhancement involves the capture of conduction band electrons by H_2O_2. In this section we describe this enhancement mechanism. The mechanism is depicted schematically in **Figure 5**.

In the absence of H_2O_2, anodic etching of Si in acidic fluoride solutions occurs by the Gerischer mechanism,[22] which can occur along a dominant valence 2 pathway and a less likely valence 4 pathway.[23,34] Therefore, the effective valence during pore formation is usually measured to be slightly above 2. There also is a valence 4 oxidation pathway that contributes to electropolishing at high current density.[16,34] The valence 2 pathway is depicted in Figure 5. Etching is initiated by hole injection into the Si valence band at the top of the figure. In step 2, a fluoride ion injects an electron into the conduction band. This "doubling electron," when measured in conjunction with the hole injected in step 1, accounts for the valence of 2. It has been shown that the balance between the valence 2 and valence 4 pathways can be altered by the reaction conditions; for example, metal catalysts induce etching with valences between 2 and 4 depending on the chemical identity of the metal.[35–37]

Even though H_2O_2 has a standard reduction potential ($E°$ = 1.775 V) that lies far below the Si valence band maximum ($E°$ ~ 0.7 V), it is unable to inject holes into the valence band at an appreciable rate compared to the rates of anodic dissolution. This is consistent both with the results we have presented

above and with literature reports.[31,32,38] The reason for this is that H_2O_2 couples very weakly to the electronic states of the Si valence band. Therefore, specific adsorption and the presence of catalytic metals are required for rapid electron transfer.[36,37]

We propose that the manner in which H_2O_2 enhances the rate of anodic dissolution is not via direct electron transfer from the valence band. Instead, the H_2O_2 enhances the etching rate by capturing the doubling electron, which resides in the conduction band. As shown in the right hand side of Figure 5, the capture of a conduction band electron will generate OH^-. Hydroxide is well known to catalyze the etching of Si by H_2O.[31,32] While this normally only occurs at high pH, in the mechanism proposed here OH^- is generated directly on the Si surface. Furthermore, the consumption of the doubling electron by the H_2O_2 means that the effective valence in the presence of both the right hand and left hand pathways will be measured as 1. Both pathways are initiated by hole injection into the valence band but neither can proceed without the adsorption of F^- and the concomitant injection of an electron into the conduction band.

3. Conclusions

We demonstrate that the rate of macropore formation by the anodization of Si in HF solutions is dramatically enhanced by the addition of H_2O_2. The enhancement facilitates the machining of structures into Si at rates that were previously unattainable. More importantly, higher etching rates are maintained during the formation of high-aspect-ratio structures compared to processes that are considered to be state-of-the-art. The rate enhancement is accompanied by a drop of the effective reaction valence to a value of 1. We propose that a parallel etching mechanism introduced by the addition of H_2O_2 is triggered by the capture of a conduction band electron released during fluoride-induced etching. This parallel pathway is responsible both for the rate enhancement and the reduction in effective valence.

4. Experimental Section

Materials and Chemicals: The starting material was a CZ-growth n-type silicon wafer with resistivity of 3–8 Ω cm, (100) oriented, phosphorous-doped, with a 298 nm thick silicon-dioxide layer on top, provided by ST Microelectronics.

HF 48 wt%, Perdrogen H_2O_2 30 wt%, pentane ($CH_3(CH_2)_3CH_3$) 99 wt%, acetone (CH_3COCH_3) 99 wt%, and 2-propanol ($(CH_3)_2CHOH$) 99.8 wt% were purchased from Sigma-Aldrich. Sodium lauryl sulfate powder ($CH_3(CH_2)_{11}OSO_3Na$) was purchased from Carlo Erba Reagents. Potassium hydroxide (KOH), pure powder at 85%, and ethanol (CH_3CH_2OH) 99.8 wt% were purchased from Fluka Analytical. Ammonium fluoride solution (NH_4F) 40 wt% was purchased from Riedel-De Haën (Aldrich).

Electrochemical Characterization of n-Type Silicon Electrode in Aqueous HF–H_2O_2 Electrolytes by Linear Sweep Voltammetry: Linear sweep voltammetry on n-type silicon electrodes in contact with aqueous HF-based electrolytes ([HF] = 5 vol%) containing different H_2O_2 concentrations (namely 0% (control), 5, 10, 20, and 25 vol%) was carried out at voltages from –1 to +2.5 V, around the OCP, under back-side illumination of the silicon at different intensity values (from 0% to 100% power of a 250 W halogen lamp). The silicon-dioxide layer on top of the silicon wafer was removed by chemical etching in HF:ethanol (1:1, v/v) before the silicon was loaded in a three-electrode electrochemical cell. Details of the electrochemical cell are provided in the Supporting Information. The *J–V* curve of the electrochemical systems under investigation was recorded by monitoring the current flowing through silicon electrode (used as the anode) and the counter electrode (i.e., a platinum disk) after applying a variable voltage in the range from +2.5 to –1 V with sweep rate of –0.1 V s^{-1} between the silicon electrode and a pseudo-reference electrode (i.e., a platinum wire). A set of three measurements was carried out for each parameter configuration.

Preparation of Regular Macropores in n-Type Silicon Electrode in Aqueous HF–H_2O_2 Electrolytes by Anodic Etching: A square hole array oriented along the (110) direction with side-to-side pitch of 3.5 µm was defined on the surface of the silicon wafer. Standard UV lithography was used to define the pattern on positive photoresist layer deposited on the silicon-dioxide surface on top of the n-type silicon wafer. The pattern was then transferred to silicon-dioxide layer by buffered hydrofluoric acid (BHF) etching using the patterned photoresist as a mask. BHF etching was performed at room temperature with a solution of HF:NH_4F (4:25, v/v). The positive photoresist layer was removed by chemical dissolution in acetone, and then the pattern was transferred to the silicon surface by KOH etching using the silicon-dioxide layer as mask, so as to create an array of inverted pyramid-shaped defects. KOH etching was performed at 50 °C in a 20% KOH solution saturated with 2-propanol to improve solution wettability and, in turn, to increase the etching uniformity. The silicon-dioxide layer was removed by chemical etching in a solution of HF:ethanol (1:1, v/v), thus leaving the patterned silicon surface uncovered. The patterned silicon samples were loaded in a three-electrode electrochemical cell and electrochemically etched under back-side illumination at constant anodic voltage of 1.2 V for different etching times, namely 10, 20, 40, and 60 s, in the presence of different aqueous electrolytes with same HF concentration ([HF] from 5 to 8 vol%) though different H_2O_2 concentrations, namely [H_2O_2] = 0% (control), 5, 10, 15, 20, and 25 vol%. In order to keep the macropore diameter constant as a function of depth, the photogenerated etching current density (J_e) was linearly decreased over time with respect to its initial value J_{e_0} = 36.49 mA cm^{-2}, which was maintained constant regardless of the electrolyte composition. Accordingly, the lamp power was reduced over time to set the decreasing rate value to –1.67 µA s^{-1} for the control solution, –1.67 µA s^{-1} for the electrolyte with [H_2O_2] = 5%, –3.44 µA s^{-1} for the electrolyte with [H_2O_2] = 10%, –4.04 µA s^{-1} for the electrolyte with [H_2O_2] = 20%, and –4.04 µA s^{-1} for the electrolyte with [H_2O_2] = 25%. The macropore growth versus time was investigated using two different methodologies: (1) a standard methodology, which required performing a number of experiments equal to the number of etching times/depths (i.e., 10, 20, 40, and 60 min) to be investigated; (2) a labeling methodology, which required performing a single experiment at the higher etching time to be investigated (i.e., 65 min) during which depth was marked over time at specific time intervals.[24] Details on the labeling methodology used in this work are provided in Supporting Information. After the electrochemical etching the microfabricated silicon samples were rinsed in deionized water, ethanol, and pentane, then dried on a hotplate at 100 °C and diced in two pieces along the (100) direction to allow morphological investigation of cross-sections.

Preparation of Microstructures in n-Type Silicon Electrode in Aqueous HF–H_2O_2 Electrolytes by Anodic Etching: Silicon microstructures integrating a 2D array of square holes with sides of about 40 µm and spatial periods of 70 µm together with a 2D array of square pores with sides of about 4 µm and spatial periods of 10 µm were pre-patterned on the surface of silicon samples according to technological steps detailed above. The larger holes were partitioned with sacrificial structures consisting of basic elements (i.e., a straight line with a suitable length of 36 µm and width 2 µm) arranged as 1D arrays of parallel lines and designed to become free-standing at the end of the electrochemical etching step. The patterned silicon samples were loaded in a three-electrode

electrochemical cell and electrochemically etched under back-side illumination at constant anodic voltage of 3 V for 10 min in an aqueous electrolyte with [HF] = 5 vol% and [H_2O_2] = 25 vol%.

The electrochemical etching consisted of a single step with an initial anisotropic phase and a final isotropic phase, both controlled by varying the etching current density (J_e) as the etching progresses.[18] During the anisotropic etching phase the pattern is deeply grooved into the silicon substrate. In this phase the J_e value was set to 103.9 mA cm^{-2} and gradually decreased over time with a slope of –11.7 µA s^{-1} for the next 10 min. During the isotropic etching phase, only silicon at the bottom of the anisotropically etched structures is etched. In this phase the J_e value was abruptly brought to a constant value of 148.4 mA cm^{-2} for 90 s so as to fully consume silicon at the bottom of sacrificial structures, which were then removed from inside the larger holes.

Investigation of Morphological Features of Regular Macropores and Microstructures: Optical (Leica Microsystems DFC295) and scanning electron (JEOL JSM-6390 at an acceleration voltage of either 3 kV or 5 kV) microscopy were used to investigate both top-view and cross-section of electrochemically etched macropore arrays and microstructures in order to probe both depth and diameter as a function of etching time and electrolyte composition.

Calculation of the Dissolution Valence of the Electrochemical Etching Process: The number of charge carriers required for the dissolution of a single silicon atom, by definition dissolution valence n, was estimated from experimental data on regular macropore etching according to the following equations

$$n = \frac{n_c}{n_{Si}} \tag{4}$$

$$n_c = \frac{A_e t_e}{2e}\left(J_{e\_0} + J_{e\_end}\right) \tag{5}$$

$$n_{Si} = V_{Si} N_{Si} \tag{6}$$

where n_c is the number of charge carriers supplied to the silicon/electrolyte system during the etching process; J_{e_0} and J_{e_end} [mA cm^{-2}] are initial and final etching current density values, respectively, used for each tested electrolyte (as detailed above); A_e [cm^2] is the area under etching of the silicon electrode; t_e [s] is the etching time; e [C] is the electron charge; n_{Si} is the total number of silicon atoms removed during the etching; V_{Si} [µm^3] is the volume of silicon removed during the etching, and N_{Si} [atom µm^{-3}] is the silicon atomic density.

Supporting Information

Supporting Information is available from the Wiley Online Library or from the author.

Acknowledgements

G.B. thanks ECSEL Joint Undertaking through the R2POWER300 project (grant No. 653933) for funding.

Received: August 20, 2016
Revised: October 21, 2016
Published online: December 12, 2016

[1] M. Lundstrom, *Science* **2013**, *299*, 210.
[2] M. M. Waldrop, *Nature* **2016**, *530*, 144.
[3] C. Monat, P. Domachuk, B. J. Eggleton, *Nat. Photonics* **2007**, *1*, 106.
[4] A. G. Krause, M. Winger, T. D. Blasius, Q. Lin, O. Painter, *Nat. Photonics* **2012**, *6*, 768.
[5] E. L. Coarer, S. Blaize, P. Benech, I. Stefanon, A. Morand, G. Lèrondel, G. Leblond, P. Kern, J. M. Fedeli, P. Royer, *Nat. Photonics* **2007**, *6*, 473.
[6] P. S. Dittrich, A. Manz, *Nat. Rev. Drug Discovery* **2006**, *5*, 210.
[7] P. Neužil, S. Giselbrecht, K. Länge, T. J. Huang, A. Manz, *Nat. Rev. Drug Discovery* **2012**, *11*, 620.
[8] A. C. Fischer, F. Forsberg, M. Lapisa, S. J. Bleiker, G. Stemme, N. Roxhed, F. Niklaus, *Microsyst. Nanoeng.* **2015**, *1*, 15005.
[9] K. Gibb, R. Krishnamurthy, *Chip Des.* **2008**, *6*, 29.
[10] W. Banqiu, A. Kumar, S. Pamarthy, **2010**, *108*, 051101; and reference within it.
[11] Y. Junghoon, Y. Wu, J. C. Selby, M. A. Shannon, *J. Vac. Sci. Technol., B* **2005**, *23*, 2319.
[12] H. Zhipeng, N. Geyer, P. Werner, J. De Boor, U. Gösele, *Adv. Mater.* **2011**, *23*, 285.
[13] S.-W. Chang, V. P. Chuang, S. T. Boles, C. A. Ross, C. V. Thompson, *Adv. Funct. Mater.* **2009**, *19*, 2495.
[14] C. Chang, A. Sakdinawat, *Nat. Commun.* **2014**, *5*, 1.
[15] L. Li, X. Zhao, C.-P. Wong, *ACS Appl. Mater. Interfaces* **2014**, *6*, 16782.
[16] V. Lehmann, *Electrochemistry of Silicon*, Wiley-VCH, Weinheim, Germany, **2002**.
[17] G. Barillaro, L. M. Strambini, *Electrochem. Commun.* **2010**, *12*, 1314.
[18] M. Bassu, S. Surdo, L. M. Strambini, G. Barillaro, *Adv. Funct. Mater.* **2012**, *22*, 1222.
[19] S. Surdo, S. Merlo, F. Carpignano, L. M. Strambini, C. Trono, A. Giannetti, F. Baldini, G. Barillaro, *Lab Chip* **2012**, *12*, 4403.
[20] G. Barillaro, *ECS Trans.* **2015**, *69*, 39.
[21] A. Cojocaru, J. Carstensen, E. K. Ossei-Wusu, M. Leisner, O. Riemenschneider, H. Foll, *Phys. Status Solidi, C* **2009**, *6*, 1571.
[22] H. Gerischer, P. Allongue, V. C. Kieling, *Phys. Chem.* **1993**, *97*, 753.
[23] K. W. Kolasinski, *Surf. Sci.* **2009**, *603*, 1904.
[24] G. Barillaro, F. Pieri, *J. Appl. Phys.* **2005**, *97*, 8.
[25] G. Polito, S. Surdo, V. Robbiano, G. Tregnago, F. Cacialli, G. Barillaro, *Adv. Opt. Mater.* **2013**, *1*, 894.
[26] V. Lehmann, *J. Electrochem. Soc.* **1993**, *140*, 2836.
[27] K. W. Kolasinski, W. B. Barclay, *Angew. Chem. Int. Ed.* **2013**, *52*, 6731.
[28] H. Föll, J. Carstensen, M. Christophersen, G. Hasse, *Phys. Status Solidi A* **2000**, *182*, 7.
[29] A. Halimaoui, *Surf. Sci.* **1994**, *306*, L550.
[30] J. Wang, H. Tu, W. Zhu, Q. Zhou, A. Liu, C. Zhang, *Mater. Sci. Eng., B* **2000**, *72*, 193.
[31] M. A. Hines, Y. J. Chabal, T. D. Harris, A. L. Harris, *J. Chem. Phys.* **1994**, *101*, 8055.
[32] T. Baum, D. J. Schiffrin, *J. Chem. Soc. Faraday Trans.* **1998**, *94*, 691.
[33] V. Bertagna, C. Plougonven, F. Rouelle, M. Chemla, *J. Electrochem. Soc.* **1996**, *143*, 3532.
[34] H. G. G. Philipsen, J. J. Kelly, *Electrochim. Acta* **2009**, *54*, 3526.
[35] E. S. Kooij, D. Vanmaekelbergh, *J. Electrochem. Soc.* **1997**, *144*, 1296.
[36] K. W. Kolasinski, W. B. Barclay, Y. Sun, M. Aindow, *Electrochim. Acta* **2015**, *158*, 219.
[37] U. Neuwald, A. Feltz, U. Memmert, R. J. Behm, *J. Appl. Phys.* **1995**, *78*, 4131.
[38] C. Gondek, M. Lippold, I. Röver, K. Bohmhammel, E. Kroke, *J. Phys. Chem., C* **2014**, *118*, 2044.